

## Probabilistic Runout Distance Analysis Using Material Point Methods

M. Lu<sup>1</sup>, M. Zhou<sup>2</sup>, and J. Zhang<sup>3</sup>

<sup>1</sup>Department of Geotechnical Engineering, Tongji University. Email: lumeng@tongji.edu.cn

<sup>2</sup>Department of Geotechnical Engineering, Tongji University. Email: zhoum@tongji.edu.cn

<sup>3</sup>Department of Geotechnical Engineering, Tongji University. Email: cezhangjie@tongji.edu.cn

**Abstract:** Probabilistically analyzing runout distance of slope failure is important for landslides risk assessment since the consequence triggered by a landslide highly depends on the runout distance of the landslide mass. Currently, the research on probabilistic analysis for runout distance after slope failure based on mechanics-based methods is limited. In this paper, an efficient assessment framework based on response surface methods and material point methods is proposed to analyze the probable runout distance of slope failure. The framework is used to study a homogeneous 2D clay slope with uncertain strength parameters, namely, the cohesion and the internal friction angle. In this case, the relationship between the factor of safety and strength parameters is approximated based on the advanced classical response surface method, and the failure domain is derived. Then, the runout distances of samples in the failure domain are calculated via the material point method. Thereafter, the kriging-based response surface method is applied to approximate relationship between the runout distance and strength parameters in the failure domain. Finally, the frequency and exceedance probability of the runout distance are computed efficiently via the two RSMs. Through statistical analysis, the number of samples that keep the slope stable is about 61.40% with respect to total number of samples. For the failed samples, the chance of the runout distance firstly increases and then decreases as the runout distance increases. The probability that the runout distance  $< 11$  m is about 99%. The proposed method provides an efficient and convenient tool to predict the probable runout distance of slope failure, and can help better assess landslide risk.

**Keywords:** Uncertainties, runout distance, slope, response surface methods, material point methods

### 1. Introduction

In the past decades, many studies have been conducted on probabilistic stability analysis of slopes (e.g., Christian et al., 1994; Ching et al., 2009; Huang et al., 2010; Gong et al., 2019), which have greatly enhanced the capability of the profession to evaluate the probability of slope failure. For quantitative risk assessment analysis, the runout distance of the slope failure should also be probabilistically analyzed, which is highly associated with the damages caused by a landslide. Currently, studies on probabilistic analysis for runout distance after slope failure based on mechanics-based methods is still limited.

In the recent years, the material point methods (MPM) developed by Sulsky et al. (1994) has been increasingly used for runout distance analysis. MPM discretizes a continuum into a set of material points and the definition of a background computational mesh can better avoid the distortion during the computation process (e.g., Andersen and Andersen, 2010; Llano-Serna et al., 2016; Soga et al., 2016). Additionally, MPM allows applying the boundary conditions relatively easily and is consistent with a common understanding of constitutive behavior (e.g., Yerro et al., 2015; Dong et al., 2017; Wang et al., 2018). Currently, the large deformation analysis of slope failure is often carried out in a deterministic way without explicit consideration of the uncertainties associated with the soil properties.

This objective of this paper is to suggest an efficient method for probabilistic analysis of the runout distance of a landslide based on MPM. The structure of this paper is as follows. Firstly, a homogeneous 2D clay slope model with uncertain strength parameters is established. Based on the advanced classical response surface method (RSM), the failure domain of the slope can be identified. Thereafter,

the runout distance of limit samples in the failure domain is analyzed based on MPM. Then, the kriging-based RSM is used to develop the relationship between the runout distance and strength parameters in the failure domain. Based on the two RSMs, the frequency and exceedance probability of the travel distance of the slope failure can be analyzed efficiently. The proposed framework provides an efficient tool to predict runout distance of slope failure probabilistically.

### 2. Study slope

A homogeneous 2D clay slope with a height of 20 m and with a slope angle of  $45^\circ$  is studied in this paper, as shown in Fig. 1.

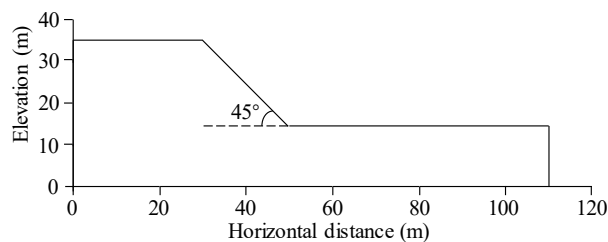


Figure 1. Geometry of the slope studied in this paper.

Let  $c$  and  $\phi$  denote the cohesion and the friction angle of the soil, respectively. The mean and standard deviation of  $c$  and  $\phi$  is summarized in Table 1. The variations of  $c$  and  $\phi$  are assumed to obey the logarithmic normal distribution. The other deterministic parameters of soil properties are also shown in Table 1. In this study, the runout distance is defined as the distance between the toe of the initial slope and the toe after slope failure (Yerro et al., 2016). The task in this example is to assess the runout distance of the slope considering the uncertainty of the soil strength parameters.

Table 1. Parameters of the soil properties.

Parameters	Value
Density (kg/m <sup>3</sup> )	1900
Elastic modulus (kPa)	5000
Poisson ratio	0.3
Tension (kPa)	0
$c$ (kPa)	Mean: 15    Std.: 3
$\phi$ (°)	Mean: 30    Std.: 6

### 3. Methodology

Runout distance analysis based on MPM is time consuming. When the slope is stable, the runout distance is zero. To reduce the computational time, we will first identify samples in the failure domain, i.e., samples with the factor of safety (FOS) less than 1.0, and will only analyse the runout distance of such samples with MPM. The traditional limit equilibrium methods or the shear strength reduction technique can be used to assess the FOS of the slope (e.g., Cheng et al., 2007; Zhang et al., 2011). When the number of samples is large and the numerical model is complex, evaluating the FOS with such methods could also be computationally expensive. To assess the runout distance efficiently, the method suggested in this paper consists of three: (1) develop the relationship between FOS and the uncertain strength parameters based on the advanced classical RSM, through which samples in the failure domain can be identified; (2) establish the relationship between the runout distance and strength parameters in the failure domain based on the kriging-based RSM; and (3) calculate distribution of the runout distance based on MCS through the use of the advanced classical RSM and the kriging-based RSM.

#### 3.1 Advanced classical RSM

Fig. 2 shows the finite difference model implemented in FLAC<sup>2D</sup>, using the elastic-perfectly plastic constitutive model described by the Mohr-Coulomb yield criterion. As the slope stability model in a homogenous soil is often quite linear, the classical RSM based on a second order polynomial can be used to model the relationship between FOS and soil parameters with reasonable (e.g., Zhang et al., 2011; Li et al., 2015). Therefore, the classical RSM will be applied. Zhang et al. (2015) suggested a method to construct the classical RSM around the design point, which is at the boundary between the stable and unstable domain. As the purpose of the current analysis is to identify soil parameters that will result in FOS < 1, we will use the method in Zhang et al. (2015) to construct the response surface. Let  $\mathbf{x}$  denote the reduced variables of  $c$  and  $\phi$ , and let  $g(\mathbf{x})$  denote the relationship between the reduced variables and FOS, which can be approximated as follows (Zhang et al., 2015):

$$g(\mathbf{x}) \approx b_0 + \sum_{i=1}^k b_i x_i + \sum_{i=k+1}^{2k} b_i x_i^2 \quad (1)$$

where  $x_i$  = the  $i$ th element of  $\mathbf{x}$ ,  $k$  = dimension of  $\mathbf{x}$ , and  $b_i$  ( $i = 0, 1, \dots, 2k$ ) = unknown deterministic coefficients. To determine the  $(2k + 1)$  coefficients, the performance function can be first evaluated around a centre point  $\mathbf{x}_c = \{x_{c1}, x_{c2}, \dots, x_{ck}\}$  and other  $2k$  points around  $\mathbf{x}_c$ :  $\{x_{c1} \pm m\sigma_{x1}, x_{c2}, \dots, x_{ck}\}$ ,  $\{x_{c1}, x_{c2} \pm m\sigma_{x2}, \dots, x_{ck}\}$ , ..., and  $\{x_{c1}, x_{c2}, \dots, x_{ck} \pm m\sigma_{xk}\}$ , where  $m$  is a parameter determining the relative distance of the calibration points and  $\sigma_{xi}$  = standard deviation of  $x_i$ . Equating the values of the performance function with those calculated using Eq. (1) at the prescribed  $(2k + 1)$  calibration points, the unknown coefficients can then be solved. In this study,  $m = 1$  is used and the FOS of calibration points are calculated based on shear strength reduction technique via FLAC<sup>2D</sup>

Let  $\mathbf{x}_D$  denote the design point found based on Eq. (1) using first-order reliability method (FORM) (Ji and Low, 2012). To construct a RSM around the design point, the response surface can be updated based on a new set of calibration points with the centre determined as follows:

$$\mathbf{x}_c = \frac{\mathbf{x}_D g(\boldsymbol{\mu}_x)}{g(\boldsymbol{\mu}_x) - g(\mathbf{x}_D)} \quad (2)$$

where  $\boldsymbol{\mu}_x$  = mean of  $\mathbf{x}$ . Eq. (1) can then be calibrated again using responses of  $g(\mathbf{x})$  evaluated at the new calibration points. Such a process is iterated until the reliability index via FORM does not change within a tolerable error  $\varepsilon_b$ . In this study,  $\varepsilon_b = 0.01$ .

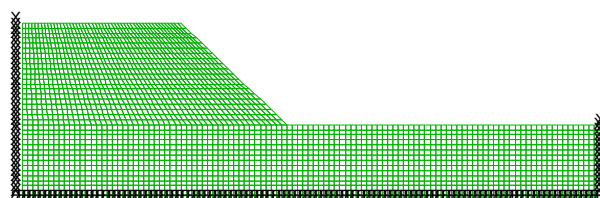


Figure 2. Slope model based on FLAC<sup>2D</sup>.

After the RSM is converged, Fig. 3 compares the FOS predicted from Eq. (1) and calculated according to FLAC<sup>2D</sup> for another 20 randomly generated combinations of  $c$  and  $\phi$ . The correlation of these two sets of FOS is 0.998, which indicates the RSM can predict the FOS of the slope with reasonable accuracy.

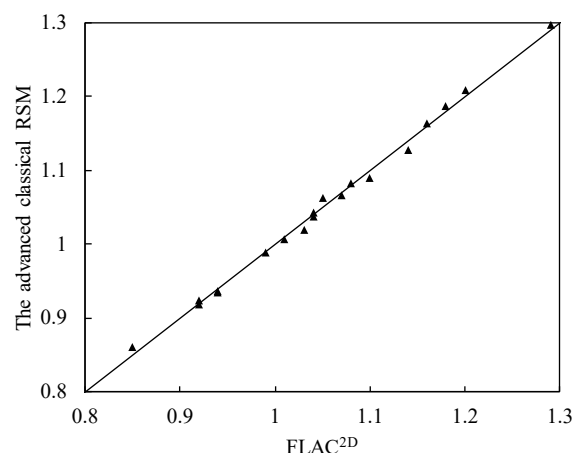


Figure 3. Comparison of FOS from the advanced classical RSM and FLAC<sup>2D</sup>.

#### 3.2 Kriging-based RSM

Based on MPM, a total number of 19640 particles are used to establish the slope model as shown in Fig. 4, with an initial particle radius of 0.5 m. The grid spacing of the

background mesh is set to be 1 m and the time step is equal to 0.2 second. The slope model via MPM uses the elastic-perfectly plastic constitutive model described by the Drucker-Prager yield criterion (e.g., Koo et al., 2017; Luo et al., 2019).

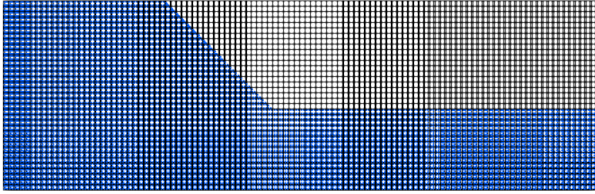


Figure 4. Slope model based on MPM.

To reduce the computational efforts involved in the MPM analysis, the kriging-based RSM is used in this study to model the relationship between the runout distance and the uncertain strength parameters in the failure domain,  $d(\mathbf{x})$ , based on samples in the failure region. In the kriging model,  $d(\mathbf{x})$  is decomposed into a deterministic trend function  $t(\mathbf{x})$  and a random error function  $\varepsilon(\mathbf{x})$  as follows (Cressie, 1993):

$$d(\mathbf{x}) = t(\mathbf{x}) + \varepsilon(\mathbf{x}) \quad (3)$$

$$E[\varepsilon(\mathbf{x})] = 0 \quad (4)$$

$$\text{COV}[\varepsilon(\mathbf{x}_i), \varepsilon(\mathbf{x}_j)] = \sigma_\varepsilon^2 R(\mathbf{x}_i - \mathbf{x}_j) \quad (5)$$

where  $\sigma_\varepsilon$  is the point standard deviation of the random function;  $\mathbf{x}_i$  and  $\mathbf{x}_j$  are two points in the parameter space and  $R(\mathbf{x}_i - \mathbf{x}_j)$  is a correlation function. In this study, the constant trend function, i.e.,  $t(\mathbf{x}) = a$ , and the Gauss correlation function are adopted as follows (Lophaven et al. 2002):

$$R(\mathbf{x}_i - \mathbf{x}_j) = \exp\left[-\sum_{m=1}^k \delta_m (x_{mi} - x_{mj})^2\right] \quad (6)$$

where  $\delta_m$  denotes a correlation parameter that reflects the degree of association between the predictions at two points along the  $m$ th axis;  $x_{mi}$  = the  $m$ th element of  $\mathbf{x}_i$ ;  $x_{mj}$  = the  $m$ th element of  $\mathbf{x}_j$ ; and  $k$  = dimension of  $\mathbf{x}$ .

To calibrate the kriging-based response surface model, 200 samples of  $\mathbf{x}$  are drawn uniformly via Latin hypercube sampling from the range defined by  $x_{i,\min} < x_i < x_{i,\max}$  ( $i = 1, 2$ ), where  $x_{i,\min}$  and  $x_{i,\max}$  are  $-4$  and  $4$ , respectively. Out of the 200 samples, 54 points are found to be in the failure domain. Then, the runout distances of these samples are analyzed based on the MPM. Based on the runout distance of these 54 samples, the kriging model can be calibrated through the maximum likelihood method (Lophaven et al., 2002). To check the accuracy of the kriging model, another 20 randomly generated samples are simulated through MPM as the test points. Fig. 5 compares the runout distances of the slope failure predicted based on the kriging model and those based on MPM. The correlation coefficient between the two sets of runout distance is 0.999, indicating the kriging model can approximate the relationship between the runout distance and uncertain strength parameters with reasonable accuracy.

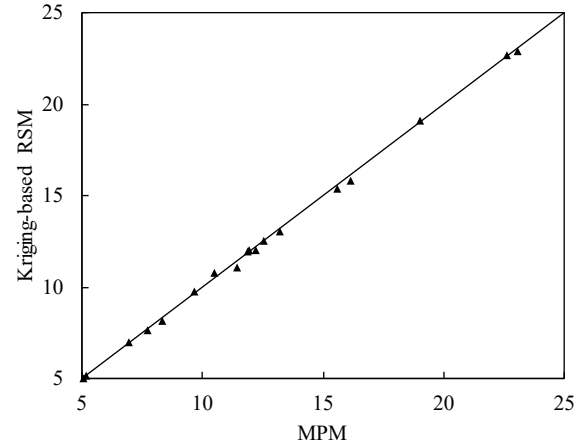


Figure 5. Comparison of runout distance from the kriging-based RSM and MPM.

## 4. Results and discussions

### 4.1 Distribution of the runout distance

10000 samples are randomly generated via MCS (Ang and Tang, 2007). Based on the two RSMs above, the runout distance of these samples can be analyzed efficiently. Through statistical analysis, the runout distance of all samples has a mean of 2.21 m and a standard deviation of 3.00 m. The number of samples with FOS > 1 accounts for 61.40% with respect to the total samples. The runout distance of these samples with FOS > 1 is assumed as 0 m.

To figure out the distribution law of the runout distance, the distributions of the failed samples between 2 m and 4 m, 4 m and 6 m, and 6 m and 8 m, are investigated as shown in Fig. 6. As can be seen from Fig. 6, the number of the failed samples between 2 m and 4 m is relatively small, accounting for 2.99% with respect to the total samples. For the failed samples between 2 m and 4 m, the cohesion is mainly in the range of 12 kPa and 16 kPa while the friction angle is mainly in the range of 27° to 31°. The number of failed samples between 4 m and 6 m is significantly larger than that between 2 m and 4 m, accounting for 25.93% with respect to total samples. This is mainly because that the range of the failed samples between 4 m and 6 m is significantly larger than that between 2 m and 4 m. For the failed samples between 4 m and 6 m, the cohesion is mainly in the range of 9 kPa and 19 kPa while the friction angle is mainly in the range of 20° to 31°. The number of failed samples between 6 m and 8 m becomes smaller comparing with that between 4 m and 6 m, accounting for 5.17% with respect to total samples. This is mainly because that the failed samples with larger runout distance are far away from the sample with mean values, hence have the smaller occurrence probability. It should be noted that there is no failed samples between 0 m and 2 m. This phenomenon is mainly induced by computational errors between FLAC<sup>2D</sup> and MPM, that the stable samples with the FOS close to 1 when calculated via FLAC<sup>2D</sup> have triggered the displacement of the slope when calculated via MPM.

According to the analysis above, it can be found that the number of failed samples firstly increases and then decreases when the runout distance increases. To clearly

illustrate this law, Fig. 7 shows the histogram of the runout distance of all samples. As can be seen from this figure, for the failed samples, the normalized frequency indeed firstly increases and then decreases when the runout distance increases and the most failed samples also fall between 4 m and 6 m. When the runout distance is larger than 12 m, the normalized frequency can be ignored.

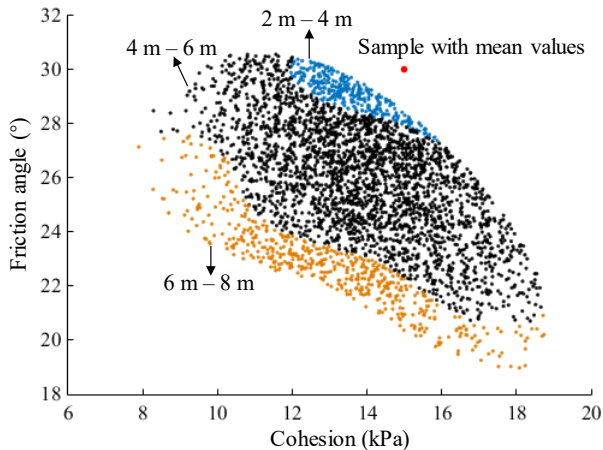


Figure 6. Distribution of failed samples between 2 m and 4 m; 4 m and 6 m; and 6 m and 8 m.

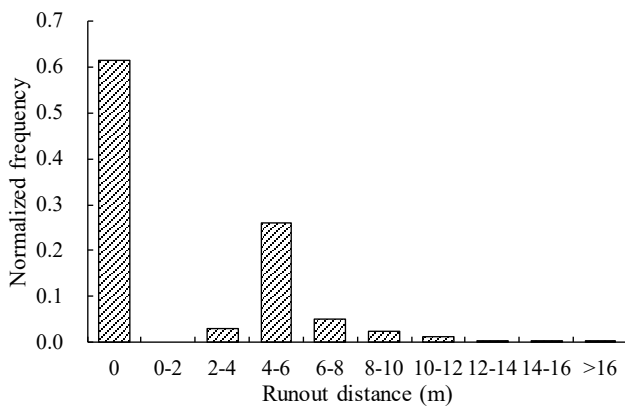


Figure 7. Histogram of the runout distance of all samples.

#### 4.2 Exceedance probability of the runout distance

Based on the obtained histogram of the runout distance, the exceedance probability of the runout distance can be also conveniently calculated, as shown in Fig. 8. As can be seen from Fig. 8, when the runout distance increases, the exceedance probability firstly remains stable and then decreases with a fast rate, which is because that the frequency of the runout distance between 0 m and 4 m is small and the frequency of runout distance between 4 m and 6 m is the largest. For the more than 6 m runout distance range, the decrease trend of the exceedance probability slows down, which is due to the decreasing of the frequency with the increasing of the runout distance. The chance of runout distance smaller than 6 m is about 90% and the chance of runout distance smaller than 11 m is about 99%. The obtained exceedance probability provides a quantitative tool for decision making in engineering practice of slope failure hazard analysis. For example, if there is a building located at 15 m away from

slope toe, the probability that sliding mass affects this building is less than 0.1 %.

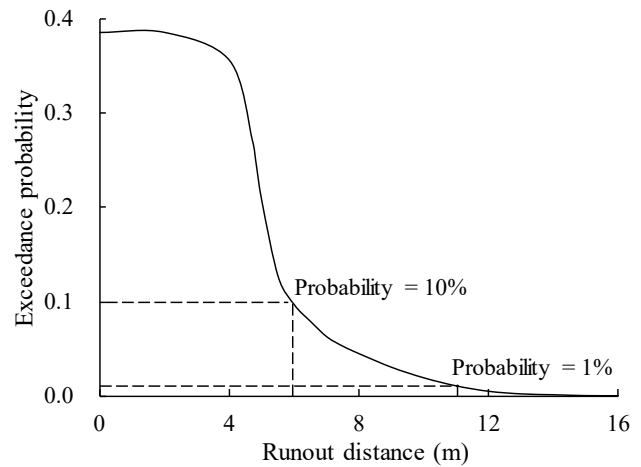


Figure 8. Exceedance probability of the runout distance.

#### 5. Conclusions

This study develops a new efficient assessment framework based on RSM and MPM for probabilistic analysis of runout distance of slope failure. A 2D homogeneous clay slope with uncertain strength parameters is studied using the proposed framework. The advanced classical RSM is suggested to identify the failure domain, and the runout distance of failed samples are analyzed based on MPM. Then, the kriging-based RSM is used to develop the relationship between the runout distance and the strength parameters in the failure domain. Based on the two RSMs, this method significantly reduces the number of samples that required for large deformation numerical simulation, which provides a computationally efficient tool to obtain the probable runout distance of slope failure associated with uncertainties. Through the proposed framework, the frequency and the exceedance probability of the runout distance can be conveniently derived. In this case, for the failed samples, the chance of the runout distance firstly increases and then decreases as the runout distance increases. The probability of the runout distance smaller than 6 m is about 90% and the probability of the runout distance smaller than 11 m is about 99%. It should be noted that the applicability of the proposed method needs two numerical simulation tools where one is to calculate FOS and another is to calculate runout distance, thus analysis results will be significantly affected by the calculation errors between the two tools. In the future studies, the relationship between FOS and runout distance obtained based on two different tools or more accurate codes of MPM should be developed to reduce the calculation errors.

#### References

- Andersen, S. and Andersen, L. 2010. Modelling of landslides with the material-point method. *Computers and Geosciences*, 14(1): 137–147.
- Ang, A.H.S. and Tang, W.H. 2007. *Probability concepts in engineering: Emphasis on applications to civil and environmental engineering*. John Wiley and Sons, New York.

- Cheng, Y.M., Lansivaara, T. and Wei, W.B. 2007. Two-dimensional slope stability analysis by limit equilibrium and strength reduction methods. *Computers and Geotechnics*, 34(3): 137–150.
- Ching, J., Phoon, K.K. and Hu, Y.G. 2009. Efficient evaluation of reliability for slopes with circular slip surfaces using importance sampling. *ASCE Journal of Geotechnical and Geoenvironmental Engineering*, 135(6): 768–777.
- Cressie, N.A.C. 1993. *Statistics for spatial data*. Wiley, New York.
- Christian, J.T., Ladd, C.C. and Baecher, G.B. 1994. Reliability applied to slope stability analysis. *Journal of Geotechnical Engineering, ASCE*, 120(12): 2180–2207.
- Dong, Y., Wang, D. and Randolph, M.F. 2017. Investigation of impact forces on pipeline by submarine landslide using material point method. *Ocean Engineering*, 146: 21–28.
- Gong, W., Tang, H., Wang, H., Wang, X. and Juang, C. 2019. Probabilistic analysis and design of stabilizing piles in slope considering stratigraphic uncertainty. *Engineering Geology*, 259: 105162.
- Huang, J., Griffiths, D.V. and Fenton, G.A. 2010. System reliability of slopes by RFEM. *Soils and Foundations*, 50(3): 343–353.
- Ji, J. and Low, B.K. 2012. Stratified response surfaces for system probabilistic evaluation of slopes. *Journal of geotechnical and geoenvironmental engineering*, 138(11): 1398–1406.
- Koo, R.C.H., Kwan, J.S., Lam, C., Goodwin, G.R., Choi, C., Ng, C.W.W., Yiu, J., Ho, K.K.S. and Pun, W.K. 2017. Back-analysis of geophysical flows using 3-dimensional runout model. *Canadian Geotechnical Journal*, 55(8): 1081–1094.
- Li, D.Q., Jiang, S.H., Cao, Z.J., Zhou, W., Zhou, C.B. and Zhang, L.M. 2015. A multiple response surface method for slope reliability analysis considering spatial variability of soil properties. *Engineering Geology*, 187: 60–72.
- Llano-Serna, M.A., Farias, M.M. and Pedroso, D.M. 2016. An assessment of the material point method for modelling large scale run-out processes in landslides. *Landslides*, 13(5): 1057–1066.
- Lophaven, S.N., Nielsen, H.B. and Søndergaard, J. 2002. DACE: A MATLAB kriging toolbox. *Technical Report IMM-TR-2002-12*, Technical University of Denmark, Denmark.
- Luo, H.Y., Zhang, L.L. and Zhang, L.M. 2019. Progressive failure of buildings under landslide impact. *Landslides*, 16(7): 1327–1340.
- Soga, K., Alonso, E., Yerro, A., Kumar, K. and Bandarda, S. 2016. Trends in large-deformation analysis of landslide mass movements with particular emphasis on the material point method. *Géotechnique*, 66(3): 248–273.
- Sulsky, D., Chenb, Z. and Schreyer, H.L. 1994. A particle method for history-dependent materials. *Computer Methods in Applied Mechanics and Engineering*, 118(1-2): 179–186.
- Wang, B., Vardon, P.J. and Hicks, M.A. 2018. Rainfall-induced slope collapse with coupled material point method. *Engineering Geology*, 239: 1–12.
- Yerro, A., Alonso, E.E. and Pinyol, N.M. 2015. The material point method for unsaturated soils. *Géotechnique*, 65(3): 201–217.
- Zhang, J., Chen, H.Z., Huang, H.W. and Luo, Z. 2015. Efficient response surface method for practical geotechnical reliability analysis. *Computers and Geotechnics*, 69: 496–505.
- Zhang, J., Zhang, L.M. and Tang, W.H. 2011. Kriging numerical models for geotechnical reliability analysis. *Soils Found*, 51(6): 1169–1177.
- Zhang, L.L., Zhang, J., Zhang, L.M. and Tang, W.H. 2011. Stability analysis of rainfall-induced slope failure: a review. *Geotechnical Engineering*, 164(164): 299–316.